

Comparative study of clean and Bi-induced (2×4) reconstruction on the InP(001) surface

A. Z. AlZahrani and G. P. Srivastava

School of Physics, University of Exeter, Stocker Road, Exeter EX4 4QL, United Kingdom

(Received 29 August 2008; revised manuscript received 8 December 2008; published 13 March 2009)

From an *ab initio* study, employing the plane-wave pseudopotential method and the density-functional scheme, we report on changes in atomic geometry, electronic states, and atomic orbitals for the clean and Bi-induced (2×4) reconstruction on the InP(001) surface. For the clean surface we have considered the well-accepted structural model characterized by an asymmetric In-P mixed dimer and a layer of threefold and fourfold In atoms. For the Bi adsorbed surface we have considered two different coverages: 0.5 and 0.25 monolayer (ML). For 0.5 ML coverage of Bi we considered two geometrical structures based on the $\alpha 2$ and $\beta 2$ models. Our calculations suggest that the $\alpha 2(2 \times 4)$ model is more stable in the P-poor/Bi-rich condition. For 0.25 ML coverage of Bi, the ground-state structure forms the $\alpha 2$ structure which is comprised of mixed Bi-P dimers in the top and third layers. These results are in agreement with the most recent core-level photoemission and scanning tunneling microscopy investigations. For both coverages the Bi/InP(001)- $\alpha 2(2 \times 4)$ system is semiconducting, characterized with smaller band gap than the clean surface.

DOI: [10.1103/PhysRevB.79.125309](https://doi.org/10.1103/PhysRevB.79.125309)

PACS number(s): 68.35.bg, 71.15.Mb, 73.20.-r

I. INTRODUCTION

III-V(001) semiconductor surfaces have been the subject of intense interest for both experimental and theoretical investigations due to their high-potential use in the development of new optoelectronic nanodevices.¹⁻⁵ The atomic geometry on these surfaces is very different from that within the corresponding bulk, leading generally to a “reconstructed” surface unit mesh.⁶ The electronic and structural properties of such surface reconstructions are species-termination dependent and are controlled by the following driving principles:⁶⁻⁸ (i) the exposed surface atoms form dimers to reduce the number of unsaturated dangling bonds, (ii) the cation dangling bonds are empty and the anion dangling bonds are doubly filled (the so-called electron-counting rule), and (iii) the resulting combination of dimers and missing dimers is arranged in such a way that the surface electrostatic energy is minimized.

Subject to the above-mentioned guiding principles, for a given species termination, the surface reconstruction is also found to depend on the atomic size of the anion, *viz.*, it is different for III-As(001), III-P(001), and III-Sb(001). The clean InP(001) surface is believed to exhibit the $(2 \times 1)/(2 \times 2)$ reconstruction for the P-rich case⁹ and the (2×4) reconstruction for the In-rich case.¹⁰⁻¹² The atomic structure of the In-rich (2×4) reconstruction varies with the heat treatment of the surface. Annealing at 400–500 °C yields the so-called $\sigma(2 \times 4)$ and $\delta(2 \times 4)$ surfaces, with In coverages of 0.75 and 0.875 monolayer (ML), respectively.¹³ In this work we restrict our attention to the surface with 0.875 ML coverage of In. From scanning tunneling microscopy (STM) and surface core-level spectroscopic investigations,¹³ the $\delta(2 \times 4)$ structure is proposed to consist of one P-In mixed dimer on the top atomic layer and four In dimers in the second atomic layer. First-principles theoretical angle-resolved photoemission spectroscopic and low-temperature reflection anisotropy spectroscopic studies¹⁴ have provided support for the $\delta(2 \times 4)$ structure.

Group V adsorbate-stabilized III-V(001) surfaces play an essential role for growing heteroepitaxial device

structures.^{15,16} This has led to a large number of investigations of atomic geometry and electronic structure of (As,Sb,Bi)/III-As(001) surfaces. From experimental point of view, the Sb/GaAs(001) surface has been extensively studied. Using reflection high-energy electron diffraction (RHEED) and core-level photoelectron spectroscopy, Maeda *et al.*¹⁶ investigated the structural properties of the Sb/GaAs(001) surface and found that when a 2×4 RHEED pattern is observed, the surface As atoms are replaced by Sb atoms. Sugiyama *et al.*¹⁷ employed the x-ray standing-wave analysis to evaluate the bond length of the resulting Sb dimer. Later, Moriarty *et al.*¹⁸ reported on details of the structural and electronic properties of the Sb/GaAs(001) using STM. In their work they proposed a structural model consisting of one Sb dimer on the top surface layer and one As dimer in the third layer. Recently, considering STM and core-level photoelectron spectroscopy, Ahola-Tuomi *et al.*¹⁹ deduced the $\alpha 2(2 \times 4)$ reconstruction for Bi/GaAs(001) for a coverage of 0.25 ML. With an increase in Bi coverage, the Bi/GaAs(001) (2×4) reconstruction was found to undergo a geometrical transition to the unusual (2×1) phase. Laukkanen *et al.*²⁰ deduced (2×6) , (2×8) , and (2×4) reconstructions with decreasing coverage for the Bi/InAs(001) surface with the help of low-energy electron diffraction (LEED), STM, and core-level photoelectron spectroscopy. Experimental studies have been complemented by several theoretical groups who have presented studies of the electronic and geometric properties of (Sb,Bi)/GaAs(001)- (2×4) surfaces. Schmidt and Bechstedt²¹ presented first-principles total-energy calculations for As- and Sb-terminated GaAs(100) (2×4) surfaces. For 0.5 ML coverage, they simulated the $\beta 2(2 \times 4)$ structure. Srivastava and Jenkins²² presented a theoretical study for Sb/GaAs(001)- (2×4) with a coverage of 0.25 ML within the $\alpha 2$ structure. Very recently, Usanmaz *et al.*²³ studied the atomic and electronic structures of 0.25 ML Bi coverage on the GaAs(001)- $\alpha 2(2 \times 4)$ surface. By considering three plausible dimer structures, Usanmaz *et al.*²³ concluded that the most stable structure consists of the top-layer As dimer replaced by Bi dimer.

Group-V/III-P(001) surfaces have received relatively less attention. Earlier, Li *et al.*²⁴ investigated the electronic and geometric properties of As/InP(001) surface using STM, LEED, and x-ray photoelectron spectroscopy (XPS). Their work suggests the formation of (4×2) , $\alpha 2(2 \times 4)$, and $\beta 2(2 \times 4)$ reconstructions for As coverages of ~ 0.25 , 0.5 , and 0.75 ML, respectively. Recently, it has been demonstrated that an ordered overlayer structure can be formed by depositing Bi on the InP(001) surface.²⁵ Deposition of about 1.5 ML of Bi at room temperature on the clean InP(001)- (2×4) surface and heating the system to around 440°C produces the Bi/InP(001)- (2×4) reconstruction with a clear LEED pattern.²⁵ This annealing temperature is close to the Bi desorption temperature of $\sim 500^\circ\text{C}$, resulting in the Bi/InP(001) surface formation with a submonolayer coverage of Bi. However, the precise coverage of Bi and detailed atomic geometry within the (2×4) unit cell have not been established. Analyses of the STM images and core-level spectra remain inclusive^{3,25} in that it is not clear whether the surface is composed of pure Bi-Bi dimers, of mixed Bi-P dimers, or of both. However, the core-level analysis by Laukkanen *et al.*²⁵ suggests that whether or not there are Bi-Bi dimers, Bi-P dimers must be present. Thus it is reasonable to conclude that although tentative structural models have been put forward for the V/InP(001) surfaces studied so far,^{3,24,25} there is in general lack of accurate determination of their atomic geometry and electronic properties.

In this work we have attempted to examine the relative stabilities of plausible geometries of Bi/InP(001)- (2×4) using the $\alpha 2$ and $\beta 2$ forms of the surface unit cell based on pure Bi-Bi and mixed Bi-P dimers. In particular, we report on a theoretical study of the atomic geometry, electronic gap states, and atomic orbitals on clean and Bi-covered InP(001)- (2×4) reconstruction with Bi coverages of 0.25 and 0.5 ML. These investigations were performed by employing the plane-wave pseudopotential scheme and local-density approximation within the density-functional theory (LDA-DFT) to the structural models proposed in the literature.

II. COMPUTATIONAL METHOD

Our studied surfaces were modeled by adopting the repeated slab method,⁶ with a supercell containing five (four) indium (phosphorus) layers and a vacuum region equivalent to four times the bulk lattice constant. The dangling bonds at the bottom In layer were saturated with fractionally charged ($Z=1.25$) pseudohydrogen atoms. The clean InP(001)- (2×4) surface was modeled by considering one mixed In-P dimer in the top atomic layer of the slab.¹⁰ The Bi/InP(001)- (2×4) surface was modeled for two Bi coverages: 0.25 and 0.5 ML. For the 0.25 ML coverage of Bi we considered two plausible models (composed of pure Bi-Bi and mixed P-Bi dimers in the first and third surface layers) based on the $\alpha 2(2 \times 4)$ structure. For the 0.5 ML coverage of Bi we also considered two different structural models. For one of these models there is a Bi-Bi dimer in each of the top and third layers, forming the $\alpha 2(2 \times 4)$ structure. In the other model we considered a $\beta 2$ -like structure composed of two Bi-Bi dimers in the top layer and one P-P dimer in the third layer.

Our calculations were performed in the framework of the density-functional theory²⁶ within the local-density approximation using our own code. For the many-body electron-electron interaction we employ the exchange and correlation potentials by Ceperley and Alder²⁷ as parametrized by Perdew and Zunger.²⁸ Electron-ion interactions were treated by using norm-conserving,²⁹ *ab initio*, fully separable pseudopotentials.³⁰ The single-particle Kohn-Sham³¹ wave functions were expanded in a plane-wave basis set with a kinetic-energy cutoff of 12 Ry. Self-consistent solutions of the Kohn-Sham equations were obtained by employing four special \mathbf{k} points³² in the irreducible part of the surface Brillouin zone. Tests runs, as well as previous work from our group, suggest that the above choices of the energy cutoff and the special \mathbf{k} points are totally adequate for the present study. During the calculations we use the calculated InP equilibrium lattice constant of 5.85 \AA . The Hellmann-Feynmann forces on ions were calculated and minimized to obtain the relaxed atomic geometry. The equilibrium atomic positions were determined by relaxing all atoms in the unit cell except the bottom In layer which was frozen into its bulk position. The average Hellmann-Feynmann force on ions and the equilibrium atomic geometry were well converged within 10 meV/\AA and $\pm 0.02 \text{ \AA}$, respectively.

III. RESULTS AND DISCUSSION

Before we study possible structures for Bi adsorption on InP(001), we will determine the structural and electronic properties of the clean surface. Under In-rich conditions, the clean InP(001) surface stabilizes with the (2×4) reconstruction. Total-energy calculations³³ suggested that the InP(001)- $\delta(2 \times 4)$ structure is the most plausible configuration for In-rich condition (0.875 ML).

A. Clean surface: δ structure

1. Atomic structure

Each surface unit cell for the InP(001)- $\delta(2 \times 4)$ structure contains one P-In mixed dimer in the top atomic layer and four exposed In dimers in the second layer. The In dimer atoms close to the P-In mixed dimer are fourfold coordinated and other In dimer atoms are threefold coordinated. The optimized geometric structure is shown in Fig. 1(a). The P-In mixed-dimer bond length, 2.57 \AA , is close to the ideal bulk bond length of 2.54 \AA and somewhat larger than the previously calculated value of 2.44 \AA by Schmidt and Bechstedt.³³ The difference in the bond length from the two calculations is actually due to the different lattice constants used in the two works. The mixed dimer is asymmetric, with a buckling of 0.44 \AA (which is in excellent agreement with 0.46 \AA obtained in the previous work³³), with a tilt angle of 11.70° . The surface-subsurface In-P bond length is very close to the surface mixed-dimer length. However, consistent with the In atomic radius, the surface-subsurface In-In bond length of 2.77 \AA is much larger than the bulk In-P bond length. This suggests a weaker surface-subsurface bonding. The vertical distance between the In atom in the mixed dimer

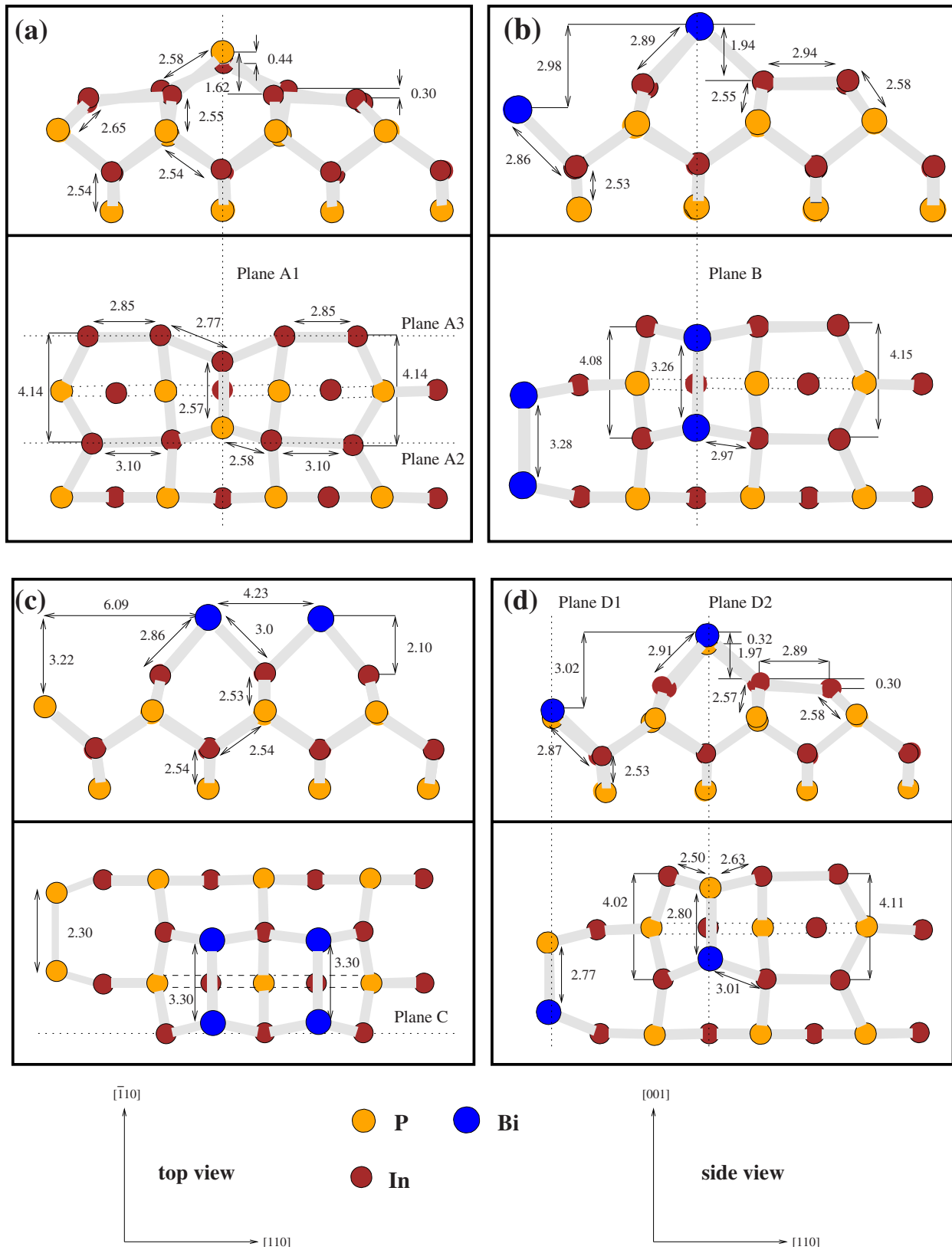


FIG. 1. (Color online) Schematic side and top views with numerical details of the optimized (a) clean InP(001) $\delta(2 \times 4)$ surface, (b) α_2 with 0.5 ML Bi coverage, (c) β_2 with 0.5 ML Bi coverage, and (d) α_2 with 0.25 ML Bi coverage. The upper and lower parts of each panel show a side view and the top view, respectively. Dotted lines represent the planes of the partial charge-density contour plots.

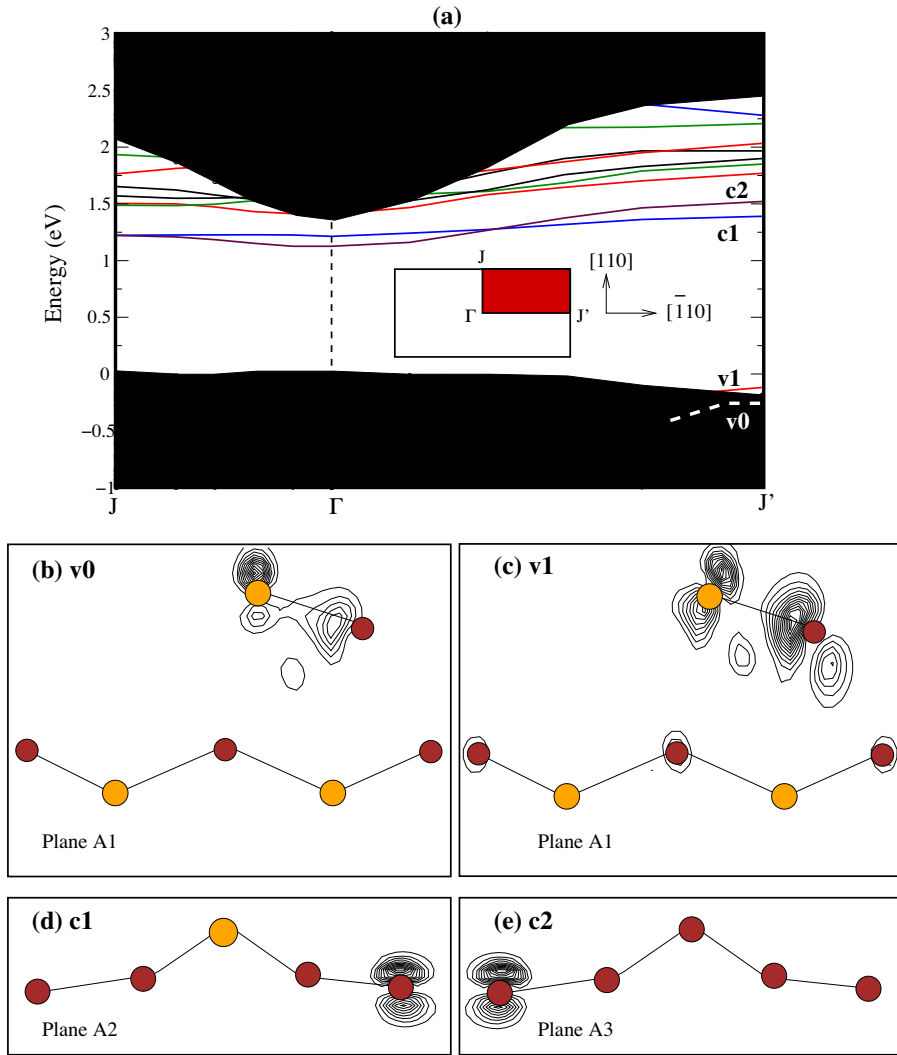


FIG. 2. (Color online) (a) Electronic band structure, near the fundamental gap, of the clean InP(001)- $\delta(2 \times 4)$ surface. The filled areas correspond to the InP projected bulk bands. Partial electronic charge density (in units of $10^{-3}e/a.u.^3$) at the J' point for (b) and (c) the highest filled states with maximum values of the density of 1.56 and 4.35, respectively, and (d) and (e) the lowest empty states with equal maximum values of the density of 2.78.

and the fourfold coordinated In atom in the second layer is 1.18 Å.

The four In dimers in the second layer are symmetrically situated with respect to the top-layer P-In mixed dimer. On each side there are two different values of the In dimer length: 2.85 and 3.10 Å on the In and P sides of the mixed dimer, respectively. The value of 2.85 Å is in good agreement with the sum of the covalent radii of In-In ($r_{In-In} = 2.88$ Å). The resulting larger bond length 3.10 Å for the second type of In dimer suggests that it is much weaker. Consistent with the threefold and fourfold coordinations of the second-layer In atoms, a buckling of 0.30 Å has been obtained in each of the In dimers. The bond lengths between the In atoms (in the second layer) and P atoms (in the third layer) are slightly different from the bulk In-P bond length. On the one hand, the bond length between the threefold coordinated In atom and P atom is increased by 0.11–2.65 Å. On the other hand, the bond length between the fourfold coordinated In atom and the P atom is 2.55 Å which is nearly equivalent to the bulk bond length. The bond length between the P atoms (in the third layer) and In atoms (in the fourth layer) is similar to the bulk bond length, 2.54 Å. These numerical results agree well with the values obtained in the previous study.³³

2. Electronic structure

The surface band structure for the clean InP(001)- $\delta(2 \times 4)$ reconstruction is given in Fig. 2(a). The shaded areas represent the projected bulk band structure of the InP(001)(2×4) reconstruction. The surface system is semiconducting, with the LDA band gap of 1.13 eV, slightly smaller than that of bulk InP. We have identified one occupied and several unoccupied surface states within the bulk InP band gap. In general, the energy locations and dispersions of these surface states are very similar to the results presented by Schmidt and Bechstedt,³³ with only minor differences.

The occupied surface state v1 is fully localized near the symmetry point J' where it lies 0.13 eV below the bulk valence-band maximum. We have identified another occupied surface state, v0, which resonates with the bulk spectrum. Both v0 and v1 originate from a linear combination of the occupied dangling orbitals at the component atoms of the P-In mixed dimer, as seen from Figs. 2(b) and 2(c). Our identification of the v0 state agrees with a similar state (v2) in the work by Schmidt and Bechstedt.³³ However, there are some disagreements between our work and that by Schmidt and Bechstedt³³ with regards to the identification of the highest occupied surface state (v1 in both our work and their

work). In the work by Schmidt and Bechstedt³³ it is found to be derived from the fourfold component of the In dimer atom. We believe that it is unlikely that a surface-localized state can originate from a fully coordinated atom. The lowest four unoccupied surface states are derived from a linear combination of the dangling-bond orbitals of the threefold coordinated In atoms at the four In dimers. This is in complete agreement with the analysis presented by Schmidt and Bechstedt.³³

B. Bi/InP(001) surface: 0.50 ML Bi coverage

STM images for 0.5 ML coverage of Bi on InP(001) have been interpreted within an $\alpha 2(2 \times 4)$ -like surface reconstruction model.³ From an analysis of core-level spectra, Laukkanen *et al.*²⁵ proposed the atomic structure within the $\alpha 2(2 \times 4)$ model of a surface unit cell. In this model the Bi atoms replace the P-In mixed-dimer atoms of the clean surface and form a symmetric Bi dimer on the top layer. Two of the four In dimers in the second atomic layer are depleted and a Bi dimer is created in the third layer. The two Bi dimers are aligned parallel to each other and are perpendicular to the remaining two In dimers. As a plausible variant of the $\alpha 2(2 \times 4)$ model, we follow the previous work done by MacPherson *et al.*¹¹ and consider the $\beta 2(2 \times 4)$ structure consisting of two parallel Bi dimers in the top layer and a P-P dimer in the third layer. In this section we have studied the atomic geometry and electronic structure of these two models. Their relative stability will be discussed in a later section.

1. $\alpha 2$ structure: Bi-Bi dimer structure

a. Atomic structure. Figure 1(b) shows the top view and a side view of the $\alpha 2$ structure of the Bi/InP(001)(2×4) surface. The Bi dimers in the top and third layers present a symmetric configuration (no vertical buckling). The Bi dimer lengths are 3.26 and 3.28 Å in the top and third atomic layers, respectively, which are close to the Bi dimer length of 3.06 Å on the Si(001) surface.³⁴ This is consistent with a previous hypothesis of the substrate independence of a dimer bond length.^{35,36} The vertical distances between the Bi atoms in the top (third) layer and the In atoms in the second (fourth) layer is 1.94 Å (1.98 Å). The surface-subsurface In-Bi bond length shows a bimodal distribution. The bond length between Bi and fourfold In, $d[\text{Bi-In}(\text{fourfold})] = 2.97$ Å, is larger than the bond length between Bi and threefold In, $d[\text{Bi-In}(\text{threefold})] = 2.89$ Å. The In-In dimer length (in the second layer) is 2.94 Å, which is only slightly smaller than the average In-In dimer length on the clean surface. The average horizontal distance between the In dimers is 4.12 Å, which is essentially the same as the value obtained for the clean surface. The In-P bond lengths below the top Bi dimer are slightly different from the bulk In-P bond length. The bond length between the fourfold In atoms and the P atoms of 2.55 Å is similar to that obtained for the clean surface. Similarly, the bond length between the threefold coordinated In atoms and the P atoms is 2.58 Å, which is quite similar to the value obtained for clean surface. The

In-P bond length below the third layer Bi dimer of 2.53 Å is again close to the bulk bond length.

b. Electronic structure. Figure 3(a) shows the electronic band structure in the vicinity of the fundamental band gap of the Bi/InP(001)- $\alpha 2(2 \times 4)$ surface, where the filled areas represent the bulk InP projected band structure. Our results indicate that the system is semiconducting with the LDA band gap of 0.80 eV, which is smaller than the band gap of the clean surface. We have identified four filled surface bands (labeled v1, v2, v3, and v4) within the fundamental gap region. These surface states are located near the Brillouin edge J' and for most part lie above the valence-band maximum (VBM). The dispersion of these states along the $\Gamma J'$ direction is generally smaller than that along the $J\Gamma$ direction. Charge-density plots of these surface states are shown in Figs. 3(b)–3(g). The v1 band originates from the p_x orbitals of the Bi dimer atoms (in both the top and third atomic layers). Figure 3(b) clarifies this for the Bi dimer atoms in the top layer. The second and third highest occupied states, v2 and v3, originate from a linear combination of the p_z dangling-bond orbitals of the Bi dimer atoms. We can interpret the orbital natures of the v2 and v3 states as π_u (bonding) and π_g (antibonding), respectively. These orbital natures are quite similar to those investigated by Gay *et al.*³⁷ for Bi on Si(001). The fourth occupied surface state, v4, is symmetrically localized around the Bi dimer atoms, showing a σ -like bond.

We have identified several empty surface states within the gap region. The surface bands labeled c1 and c2 are essentially the same as shown in Fig. 2(a) for the clean InP(001)(2×4) surface and originate from a linear combination of the dangling-bond orbitals of the threefold coordinated In atoms at the remaining two In dimers. To clarify this, we have shown the charge-density plot for the c1 state in Fig. 3(f). The surface state labeled c3 is more dispersive along the $\Gamma J'$ direction and is made of the $p_y p_y \sigma^*$ orbital from the Bi dimer atoms as shown in Fig. 3(g).

Moreover, we have simulated a STM image of the Bi/InP(001)- $\alpha 2(2 \times 4)$ surface. Our theoretical STM images are performed using the Tersoff-Hamann method³⁸ in the constant-height mode. The tunneling current is derived from the local density of states close to the Fermi energy E_F . Using this model, we simulate the filled-state image from the electronic energy calculations by integrating over the energy range E_F to $E_F + eV_B$, where V_B is the bias voltage. Figure 4 shows the simulated STM image for the occupied states with a bias of -2.0 eV. We can clearly observe two rows of bright protrusion (shown in red and light green in the online version) along the Bi dimer lines. There is a bright, but broad, protrusion on and around the top-layer Bi dimers. The brightest part of this comes from the top-layer Bi dimer atoms. A detailed image of the top surface layer is presented in the bottom panel, clearly showing Bi dimer formation. The brightness around the Bi dimers originates from the fourfold In atoms to which the Bi dimer atoms are bonded. The asymmetry of features around this bright region is consistent with the arrangement of atoms around the top-layer Bi dimer at-

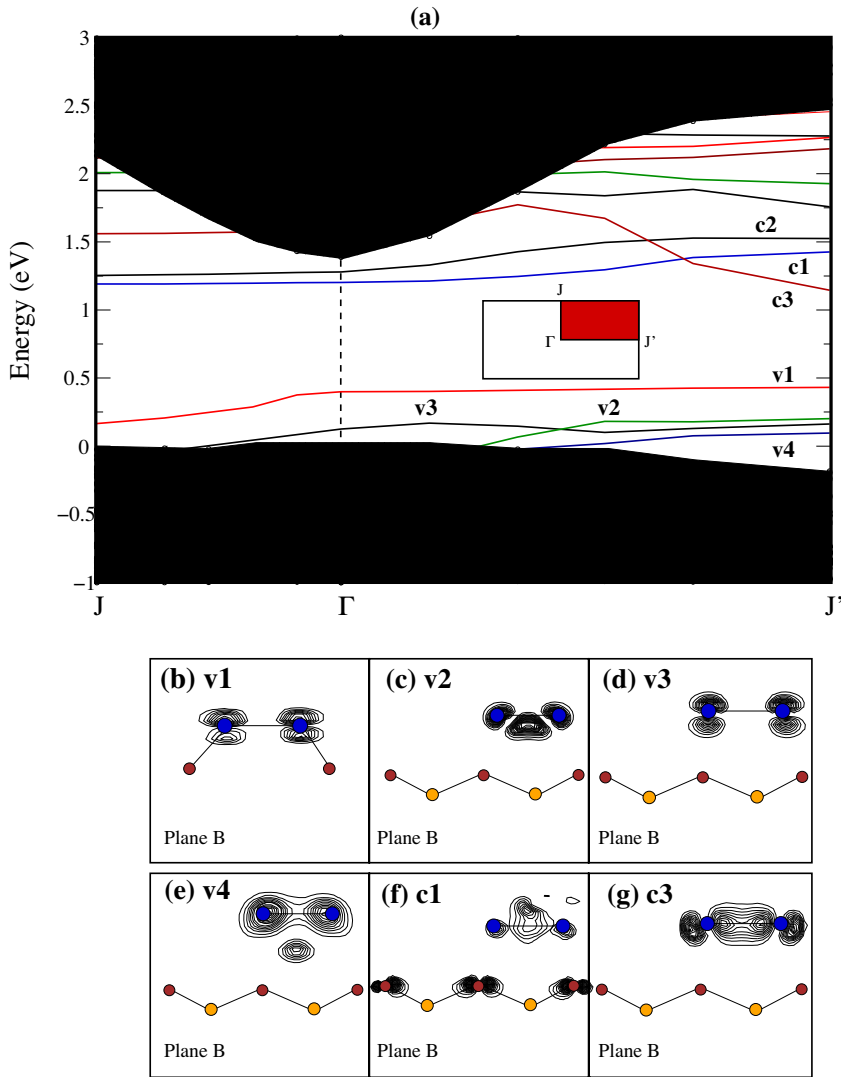


FIG. 3. (Color online) (a) Electronic band structure, near the fundamental gap, of the InP(001)- $\alpha 2(2 \times 4)$ surface with Bi coverage of 0.5 ML. The filled areas correspond to the InP projected bulk bands. Partial electronic charge density in units of ($10^{-3}e/a.u.^3$) at the J' point for (b)–(e) the highest filled states with maximum values of the density of 4.2, 6.58, 6.40, and 1.78, respectively, and (f) and (g) the lowest empty states with maximum values of the density of 1.67 and 5.63, respectively.

oms. The narrower and less brighter protrusion (light green in the online version) results from the third-layer Bi dimer atoms. Consistent with the geometry of the unit cell, this row of protrusion is asymmetrically located between two brighter rows of protrusion. These features in our theoretically simulated STM images are totally consistent with the experimental STM images obtained by Laukkanen *et al.*³ [denoted as Fig. 4(b) in their work]. The experimental images also show two rows of protrusion with different brightness. Broad white paired maxima were related to the first-layer Bi dimer atoms. Narrower rows of gray maxima, located asymmetrically between the rows of the white features, were assigned to the third-layer Bi dimers.

2. $\beta 2$ structure

a. Atomic structure. Following the previous studies carried out by Broekman *et al.*³⁹ for the As-rich GaAs(001): $\beta 2-(2 \times 4)$ model and MacPherson *et al.*¹¹ for a P-terminated two dimer-two missing dimer InP(001)(2×4) model, we have considered a $\beta 2$ -like structural model composed of two parallel Bi-Bi dimers in the top surface layer and one P-P dimer in the third layer of the InP(001)(2×4)

surface unit cell. Figure 1(c) exhibits the geometrical model and details of the equilibrium atomic geometry for this structure. In this model, the separation between the Bi dimers is calculated to be 4.23 Å. The Bi-Bi dimer bond length is 3.30 Å which is much larger than twice the Bi covalent radius and very comparable with that of the $\alpha 2$ structure. This increase in length leads to weakness of the bond. In the second layer, there are six In atoms: four of them are aside the Bi dimers (two on each side) whereas two are in the middle of the dimers. The bond length between the Bi atoms and the In atoms (aside the dimers) is 2.86 Å, which is very close to the value obtained for the $\alpha 2$ structure. This bond length increases to 3.0 Å for the In atoms in the middle of the Bi-Bi dimers. The vertical height between the Bi-Bi dimers and the subsurface In atomic layer of 2.10 Å is slightly larger than calculated distance for the $\alpha 2$ structure. The In-P bond length is 2.53 Å, which is quite similar to the ideal bulk bond length. The P-P dimer length in the third layer is 2.30 Å, which is approximately 8% larger than twice the covalent radius of the P atom.

b. Electronic structure. In Fig. 5(a) the bound surface-state energy bands of the $\beta 2$ -like model along the high-

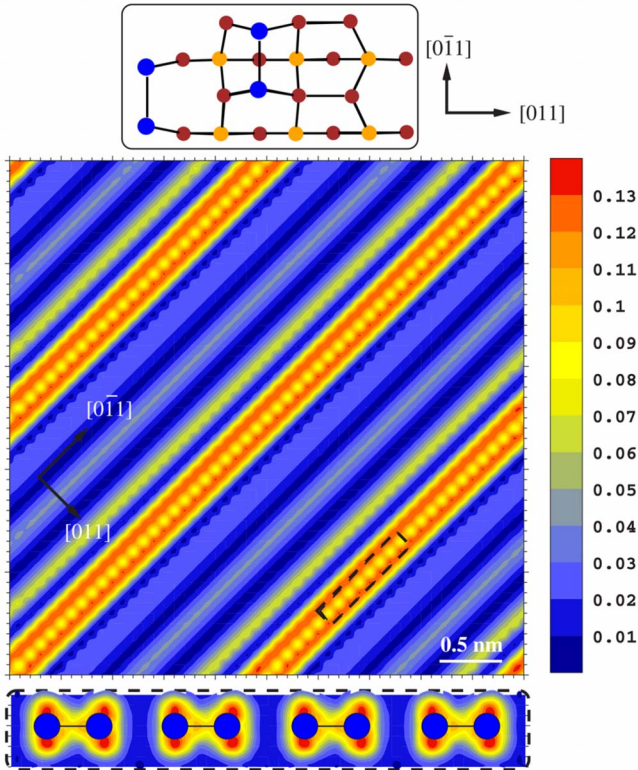


FIG. 4. (Color online) Simulated STM image for the filled states of the Bi/InP(001) α_2 -(2 \times 4) surface with a bias of 2.0 eV below the Fermi energy. The associated bar (right) represents the minimum and maximum density in terms of $e/a.u.^3$. The bottom panel shows a detailed image of the top Bi dimer layer. The top view of the surface unit cell is shown in the top panel.

symmetry directions on the surface Brillouin zone (J - Γ - J') are shown together with the projected InP bulk band structure. Eight surface states have been identified to lie within the bulk band-gap region. The second lower occupied surface state, v_2 , has its maximum at the J' point, 0.05 eV below the bulk valence-band edge. The orbital nature of this surface state arises from $pp\sigma^*$ due to the Bi atoms in the top layer as shown in Fig. 5(c). The unoccupied surface bands are entirely empty. However, the lowest band (labeled c_1) is partially filled, thus causing metallicity of the surface. The partially filled state, c_1 , and the highest occupied state, v_1 , are degenerate at the J' and have been identified to originate from the dangling bonds of the Bi dimer atoms in the top layer with a weak $pp\sigma$ orbital nature. The second highest unoccupied state, c_2 , is related to the Bi dangling bond.

C. Bi/InP(001) surface: 0.25 ML coverage

Similar to Bi(0.5 ML)/InP(001), STM images for 0.25 ML coverage of Bi on GaAs $_x$ N $_{1-x}$ (001) surfaces also indicate an α_2 -(2 \times 4)-like surface reconstruction.³ From an analysis of core-level spectra, Laukkanen *et al.*²⁵ proposed three possible atomic geometrical models within each (2 \times 4) surface unit cell for Bi(0.25 ML)/InP(001). These are based on (i) one Bi-Bi dimer on the top layer and one P-P dimer in the third

layer, (ii) one Bi-Bi dimer in the third layer and one P-P dimer in the top layer, and (iii) Bi-P mixed dimers in the top and third layers. Although the tentative conclusion of the work carried out by Laukkanen *et al.*²⁵ is that the Bi-P mixed dimers is the most plausible, this remains to be confirmed. Recently, from *ab initio* calculations for Bi(0.25 ML)/GaAs(001) α_2 -(2 \times 4), Usanmaz *et al.*²³ concluded that configuration (ii) is much less likely to occur than configuration (i). With the above results and analyses in mind, in the present study we have modeled two structures for Bi(0.25 ML)/InP(001) α_2 -(2 \times 4). In the first model, we have considered one Bi-Bi dimer at the top layer and one P-P dimer in the third layer. For the second model, we have replaced the Bi-Bi dimer in the top layer and P-P dimer in the third layer by Bi-P mixed dimers. Our total-energy calculations indicate that the Bi-P dimer structure (second model) is energetically more plausible than the first structure by approximately 0.23 eV/(1 \times 1) unit cell. For this reason, we have only detailed the results for the second model.

α_2 structure: Bi-P mixed-dimer structure

a. Atomic structure. The optimized geometry for the most stable model (Bi-P dimer structure) of the Bi-adsorbed InP(001) surface is schematically shown in Fig. 1(d). Our calculated Bi-P dimer bond lengths are 2.80 and 2.77 Å for the first and third layers, respectively. The mixed Bi-P dimer, in both the top layer and the third layer, is asymmetric, with Bi (P) in up (down) position and a tilt of 0.32 Å. The relative heights of the P and Bi atoms, as well as the magnitude of the tilt, in the mixed Bi-P dimer are governed by a combination of the electronegativity difference between P and Bi and available strain relieving mechanisms. The electronegativity difference between P and Bi should favor the P atom to be the upper component of the dimer. However, it appears that the size difference between the Bi and P atoms as well as the conservation of the atomic bond lengths formed between the dimer atoms and the atoms in the second layer have provided a huge strain relieving mechanism in an overall favor of the Bi (up)-P (down) dimer configuration. A similar situation was found by Usanmaz *et al.*²³ in their study of the Bi/GaAs(001)- α_2 (2 \times 4) system.

Similar to what is found for the Bi-Bi dimer structure, we find that for the Bi-P dimer structure the surface-subsurface In-Bi bond length also shows a bimodal distribution. The bond length between Bi and fourfold In, $d[\text{Bi-In}(\text{fourfold})] = 3.01$ Å, is larger than the bond length between Bi and threefold In, $d[\text{Bi-In}(\text{threefold})] = 2.91$ Å. We also find a similar bimodal bond-length distribution involving the P atom of the mixed dimer: the bond length between P and fourfold In, $d[\text{P-In}(\text{fourfold})] = 2.63$ Å, is larger than the bond length between P and threefold In, $d[\text{P-In}(\text{threefold})] = 2.50$ Å.

The presence of the mixed Bi-P dimer on the top layer has resulted in the In-In dimers in the second atomic layer to become asymmetric and shorter, with a buckling of 0.30 Å and a bond length of 2.89 Å. The average horizontal separation between the In dimers is reduced, compared to the Bi-Bi dimer structure, to 4.07 Å. However, our calculated vertical separation between the Bi dimer component and the

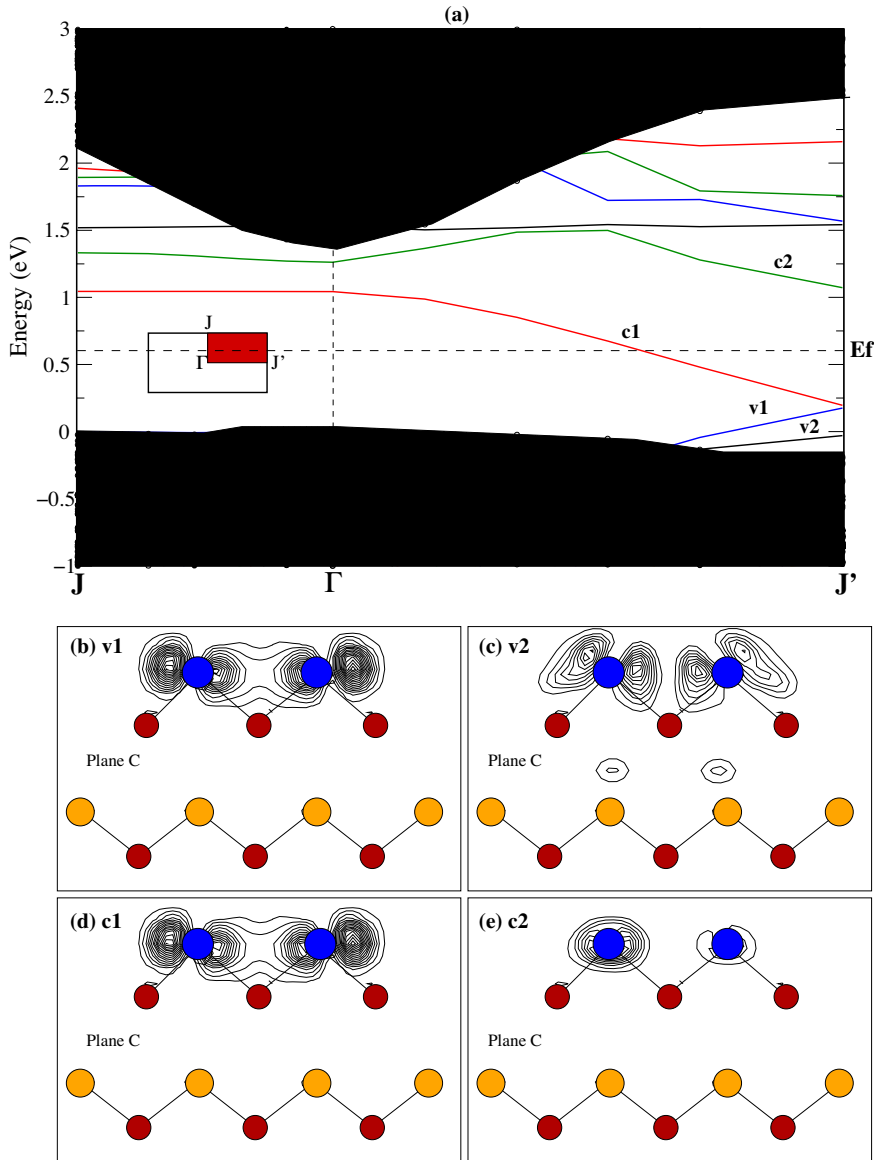


FIG. 5. (Color online) (a) Surface electronic band structure, near the fundamental gap, of the InP(001)- $\beta 2(2 \times 4)$ surface. The filled areas correspond to the InP projected bulk bands. Partial electronic charge density ($10^{-3}e/a.u.^3$) at the J' point for (b) and (c) the highest filled states with maximum values of the density of 3.26 and 2.68, respectively, and (d) and (e) the lowest empty states with maximum values of the density of 3.26 and 0.87, respectively.

In atomic layer is 1.97 Å, which is quite similar to the value obtained for the Bi-Bi dimer structure. The vertical separation between the mixed dimers in the top and third layers is 3.02 Å (from Bi to Bi). This value is quite comparable with that obtained for the Bi-Bi dimer structure. The bond length between In atoms (either fourfold or threefold in the second atomic layer) and P atoms (in the third atomic layer) is 2.57 Å, which is nearly identical to the value obtained for the Bi-Bi dimer structure.

b. Electronic structure. Figure 6(a) shows the electronic band structure of the Bi-P dimer structure. Compared to the Bi-Bi dimer structure, there are significant changes in the number of gap states and their dispersion. The orbital characteristics of some of these surface states are shown in Figs. 6(b)–6(e). The calculated surface LDA band gap is approximately 1.0 eV, which is higher than the calculated surface band gap for the Bi-Bi dimer structure for 0.5 ML coverage. We have identified two closely lying filled electronic surface states (labeled v1 and v2) within the gap region between the bulk valence and conduction bands. These surface states are

primarily localized for \mathbf{k} points close to the J' point. The highest occupied state, v1, originates from the third-layer mixed dimer with a π_g -like bonding configuration [Fig. 6(b)]. The second highest occupied state, v2, originates from the upper component of the top-layer mixed dimer [Fig. 6(c)]. The lowest two unoccupied states (labeled c1 and c2) are nearly degenerate at the J' point. The partial charge-density plots at J' show that these states are contributed from orbitals (p_y and p_z) of the mixed-dimer atoms and p_y orbitals of the threefold In atoms.

D. Comparative discussion of the three reconstructions for 0.25 and 0.5 ML Bi coverages

Using our theoretical method we can examine the relative stabilities of the $\alpha 2$ and $\beta 2$ reconstructions for the 0.25 and 0.5 ML Bi coverages. We express the surface formation energy ΔE_s as

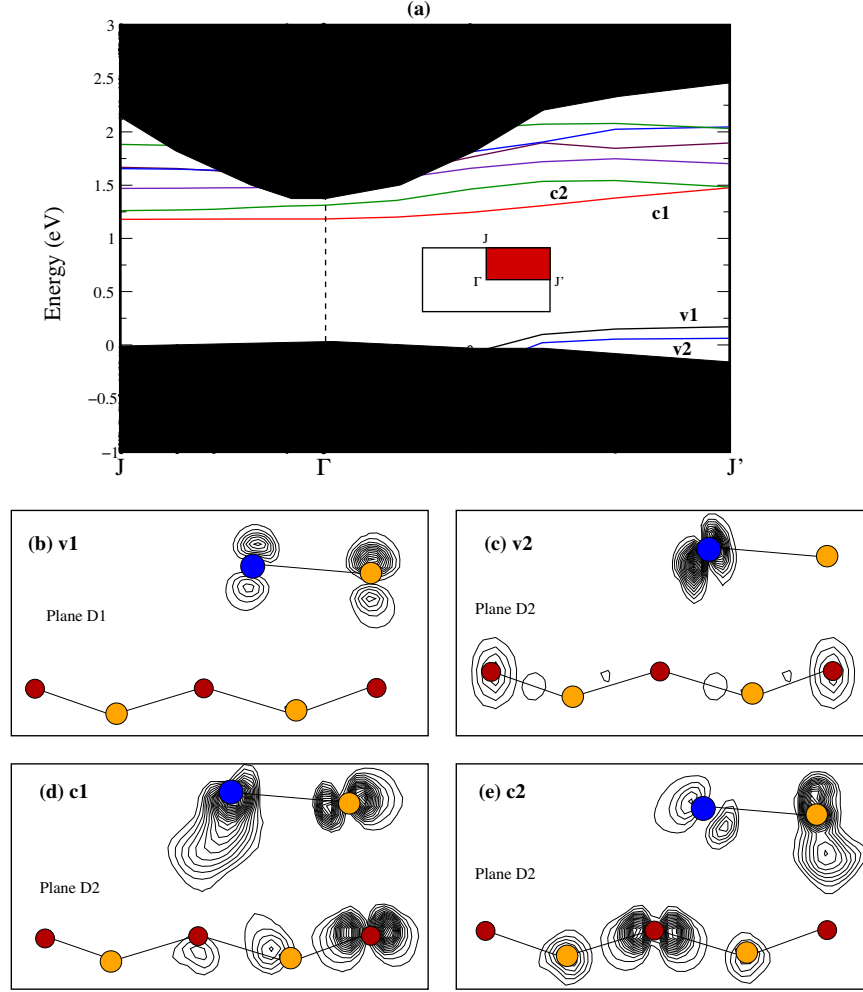


FIG. 6. (Color online) (a) Electronic band structure, near the fundamental gap, of the InP(001)- $\alpha 2(2 \times 4)$ surface with Bi coverage of 0.25 ML. The filled areas correspond to the InP projected bulk bands. Partial electronic charge density ($10^{-3} e/a.u.^3$) at the J' point for (b) and (c) the highest filled states with maximum values of the density of 2.45 and 3.21, respectively and (d) and (e) the lowest empty states with maximum values of the density of 4.54 and 4.42, respectively.

$$\Delta E_s = E_n - E_{\text{ref}} - \Delta N_P \Delta \mu_P - \Delta N_P \mu_P^{\text{bulk}} - \Delta N_{\text{Bi}} \Delta \mu_{\text{Bi}} - \Delta N_{\text{Bi}} \mu_{\text{Bi}}^{\text{bulk}}, \quad (1)$$

where E_n is the total energy of the reconstruction, E_{ref} is taken as the total energy of the clean InP(001)- $\delta(2 \times 4)$ surface, and ΔN_P and ΔN_{Bi} are the difference of P and Bi atoms, respectively. The symbols μ_P and μ_{Bi} indicate the atomic chemical potentials for P and Bi species. We determined μ_P^{bulk} and $\mu_{\text{Bi}}^{\text{bulk}}$ from bulk calculations for P and Bi in the monoclinic and rhombohedral structures, respectively.

Using the results for ΔE_s , we have plotted in Fig. 7 a phase diagram including all the three Bi-induced reconstructions and the clean surface as a function of P- and Bi-chemical potentials. In the extreme Bi-poor/P-poor limit, the clean surface is clearly indicated as the most stable phase. Under the P-rich/Bi-poor condition, $\alpha 2:0.25$ ML is the most stable phase among the three different structures. Under the P-poor/Bi-rich condition, the $\alpha 2:0.5$ ML structure is more stable than the $\beta 2:0.5$ ML structure. This conclusion is supported by the structure proposed by Laukkanen²⁵ using the core-

level photoemission spectroscopy. This situation is different from the 0.5 ML coverages of As and Sb on GaAs(001), for which Schmidt and Bechstedt²¹ modeled the $\beta 2$ structure. However, the $\beta 2:0.5$ ML becomes more stable under the P-rich/Bi-rich condition.

IV. SUMMARY AND CONCLUSION

We have performed a detailed study of the atomic geometries, electronic states, and atomic orbitals of the clean and three different Bi-covered InP(001)(2×4) surfaces using first-principles total-energy calculations. Our results for the clean surface, characterized by the topmost asymmetric mixed dimer as well as threefold and fourfold coordinated In atoms forming four In dimers, are in good agreement with previously published works. The clean surface is semiconducting, with the LDA Kohn-Sham band gap of 1.13 eV slightly smaller than the band gap of bulk InP. Within the InP band gap, the highest occupied surface state originates from the mixed In-P dimer, and the lowest unoccupied state origi-

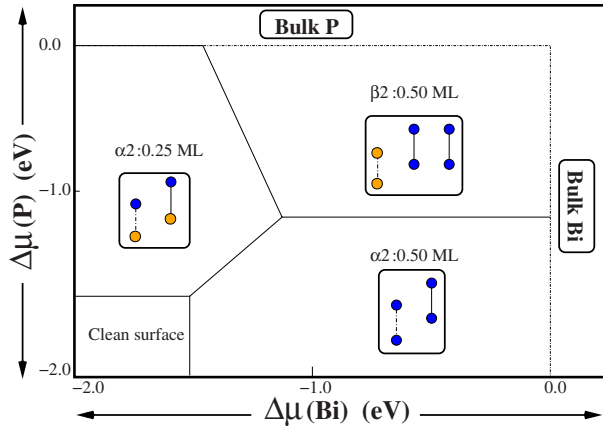


FIG. 7. (Color online) A phase diagram of the formation energy for the $\alpha 2$ - and $\beta 2$ -(2×4) structural models for 0.25 and 0.5 ML Bi coverages of InP(001). The range of the chemical potentials of P and Bi is related to their bulk values.

nates from the threefold coordinated In atoms in the second layer.

For 0.5 ML coverage of Bi we considered two geometrical models based on the $\alpha 2$ and $\beta 2$ structures. In contrast to the previously accepted $\beta 2$ model for As and Sb overlayers on GaAs(001),²¹ our work suggests that it is the $\alpha 2$ model that provides the stable structure for Bi/InP(001). Under the P-poor/Bi-rich condition, the $\alpha 2$ structure becomes more stable than the $\beta 2$ structure. While the $\beta 2$ structure is metallic, the Bi/InP(001)- $\alpha 2(2 \times 4)$ system is semiconducting,

with the LDA Kohn-Sham band gap of 0.8 eV. The highest occupied surface state originates from the lone p_z orbitals at the Bi dimer atoms. There are three closely lying unoccupied states, with the lowest (c3) originating from the $pp\sigma^*$ orbital at the Bi dimer.

We also examined two geometrical models for 0.25 ML coverage of Bi. Both form the $\alpha 2$ structure, one comprised of pure Bi-Bi and P-P dimers in the top and third layers, respectively, and the other comprised of mixed Bi-P dimers in the top and third layers. The second model is found to be more stable. This is in contrast to Sb/GaAs(001) for which the generally accepted model is comprised of pure dimers in the top and third layers.^{18,36} This is also different from Bi/GaAs(001) for which the pure dimers structure is slightly more stable than the mixed-dimers structure.²³ The mixed-dimer model is semiconducting, with the LDA band gap of 1.0 eV. The highest occupied state originates from the third-layer mixed dimer with a π_g -like bonding configuration. The lowest two unoccupied states (labeled c1 and c2) are nearly degenerate at the J' point and contributed from orbitals (p_y and p_z) of the mixed-dimer atoms and p_y orbitals of the threefold In atoms.

ACKNOWLEDGMENTS

A. Z. AlZahrani gratefully acknowledges financial support from King Abdulaziz University (KAU), Saudi Arabia. The calculations reported here were performed using the University of Exeter's SGI Altix ICE 8200 supercomputer.

- ¹M. Ahola-Tuomi, P. Laukkanen, M. Punkkinen, R. Perälä, I. Väyrynen, M. Kuzmin, K. Schulte, and M. Pessa, *Appl. Phys. Lett.* **92**, 011926 (2008).
- ²H. Sahaf, L. Masson, C. Leandri, B. Aufary, G. Lay, and F. Ronci, *Appl. Phys. Lett.* **90**, 263110 (2007).
- ³P. Laukkanen, J. Pakarinen, M. Ahola-Tuomi, M. Kuzmin, R. E. Perälä, I. J. Väyrynen, A. Tukiainen, J. Konttinen, P. Tuomisto, and M. Pessa, *Phys. Rev. B* **74**, 155302 (2006).
- ⁴O. Gurlu, O. Adam, H. Zandvliet, and B. Poelsema, *Appl. Phys. Lett.* **83**, 4610 (2003).
- ⁵J. Li, X. Liang, J. Jia, X. Liu, J. Wang, E. Wang, and Q. Xue, *Appl. Phys. Lett.* **79**, 2826 (2001).
- ⁶G. P. Srivastava, *Theoretical Modeling of Semiconductor Surfaces* (World Scientific, Singapore, 1999).
- ⁷M. D. Pashley, *Phys. Rev. B* **40**, 10481 (1989).
- ⁸C. B. Duke, *Chem. Rev. (Washington, D.C.)* **96**, 1237 (1996).
- ⁹L. Li, B.-K. Han, Q. Fu, and R. F. Hicks, *Phys. Rev. Lett.* **82**, 1879 (1999).
- ¹⁰M. M. Sung, C. Kim, H. Bu, D. S. Karpuzov, and J. W. Rabalais, *Surf. Sci.* **322**, 116 (1995).
- ¹¹C. D. MacPherson, R. A. Wolkow, C. E. J. Mitchell, and A. B. McLean, *Phys. Rev. Lett.* **77**, 691 (1996).
- ¹²K. B. Ozanyan, P. J. Parbrook, M. Hopkinson, C. R. Whitehouse, Z. Sobiesierski, and D. I. Westwood, *J. Appl. Phys.* **82**, 474 (1997).

- ¹³L. Li, Q. Fu, C. H. Li, B.-K. Han, and R. F. Hicks, *Phys. Rev. B* **61**, 10223 (2000).
- ¹⁴W. G. Schmidt, N. Esser, A. M. Frisch, P. Vogt, J. Bernholc, F. Bechstedt, M. Zorn, Th. Hannappel, S. Visbeck, F. Willig, and W. Richter, *Phys. Rev. B* **61**, R16335 (2000).
- ¹⁵B. Noshov, W. Weinberg, W. Barvosa-Carter, B. Bennett, B. Shanabrook, and L. Whitman, *Appl. Phys. Lett.* **74**, 1704 (1999).
- ¹⁶F. Maeda, Y. Watanabe, and M. Oshima, *Phys. Rev. B* **48**, 14733 (1993).
- ¹⁷M. Sugiyama, S. Maeyama, F. Maeda, and M. Oshima, *Phys. Rev. B* **52**, 2678 (1995).
- ¹⁸P. Moriarty, P. H. Beton, Y.-R. Ma, M. Henini, and D. A. Woolf, *Phys. Rev. B* **53**, R16148 (1996).
- ¹⁹M. Ahola-Tuomi, P. Laukkanen, R. Perälä, M. Kuzmin, J. Pakarinen, I. Väyrynen, and M. Adell, *Surf. Sci.* **600**, 2349 (2006).
- ²⁰P. Laukkanen, M. Ahola-Tuomi, M. Kuzmin, R. Perälä, I. Väyrynen, and J. Sadowski, *Surf. Sci.* **598**, L361 (2005).
- ²¹W. G. Schmidt and F. Bechstedt, *Surf. Sci.* **377-379**, 11 (1997).
- ²²G. P. Srivastava and S. J. Jenkins, *Surf. Sci.* **377-379**, 23 (1997).
- ²³D. Usanmaz, M. Çakmak, and Ş. Ellialtıođlu, *J. Phys.: Condens. Matter* **20**, 265003 (2008).
- ²⁴C. H. Li, L. Li, D. C. Law, S. B. Visbeck, and R. F. Hicks, *Phys. Rev. B* **65**, 205322 (2002).
- ²⁵P. Laukkanen, M. Ahola-Tuomi, J. Adell, M. Adell, K. Schulte, M. Kuzmin, M. Punkkinen, J. Pakarinen, A. Tukiainen, R.

- Perälä, I. Väyrynen, and M. Pessa, *Surf. Sci.* **601**, 3395 (2007).
- ²⁶P. Hohenberg and W. Kohn, *Phys. Rev.* **136**, B864 (1964).
- ²⁷D. M. Ceperley and B. J. Alder, *Phys. Rev. Lett.* **45**, 566 (1980).
- ²⁸J. P. Perdew and A. Zunger, *Phys. Rev. B* **23**, 5048 (1981).
- ²⁹X. Gonze, R. Stumpf, and M. Scheffler, *Phys. Rev. B* **44**, 8503 (1991).
- ³⁰L. Kleinman and D. M. Bylander, *Phys. Rev. Lett.* **48**, 1425 (1982).
- ³¹W. Kohn and L. Sham, *Phys. Rev.* **140**, A1133 (1965).
- ³²H. J. Monkhorst and J. D. Pack, *Phys. Rev. B* **13**, 5188 (1976).
- ³³W. Schmidt and F. Bechstedt, *Surf. Sci.* **409**, 474 (1998).
- ³⁴S. C. A. Gay and G. P. Srivastava, *Phys. Rev. B* **61**, 2688 (2000).
- ³⁵S. J. Jenkins and G. P. Srivastava, *J. Phys.: Condens. Matter* **8**, 6641 (1996).
- ³⁶S. J. Jenkins and G. P. Srivastava, *Phys. Rev. B* **56**, 9221 (1997).
- ³⁷S. C. Gay, S. J. Jenkins, and G. P. Srivastava, *J. Phys.: Condens. Matter* **10**, 7751 (1998).
- ³⁸J. Tersoff and D. R. Hamann, *Phys. Rev. B* **31**, 805 (1985).
- ³⁹L. Broekman, R. Leckey, J. Riley, B. Usher, and B. Sexton, *Surf. Sci.* **331-333**, 1115 (1995).